



An insight into a base-free Michael addition reaction as catalyzed by a bifunctional nickel N-heterocyclic carbene complex using density functional theory studies

Madanakrishna Katari, Gopalan Rajaraman*, Prasenjit Ghosh*

Department of Chemistry, Indian Institute of Technology Bombay, Powai, Mumbai 400 076, India



ARTICLE INFO

Article history:

Received 23 October 2013

Received in revised form

18 February 2014

Accepted 20 February 2014

Available online 13 March 2014

Keywords:

Nickel

N-Heterocyclic carbene

Michael reaction

Base-free

DFT studies

ABSTRACT

A proposed catalytic pathway for a base-free Michael addition reaction mediated by a *N/O*-functionalized *N*-heterocyclic carbene (NHC) based bifunctional nickel precatalyst has been probed using density functional theory (DFT) studies. In particular, the base-free Michael addition of a β -dicarbonyl compound namely, 2-acetyl-cyclopentanone (**a**) with methyl vinyl ketone (**b**) as catalyzed by a representative bifunctional nickel precatalyst viz. [1-(Me)-3-*N*-(methylacetamido)imidazol-2-ylidene]₂Ni (**A**) has been investigated. The modeling studies reveal that the nucleophilic attack of a metal bound enolate moiety of a 1,3-dicarbonyl adduct species (**B**) to the approaching activated olefinic substrate, methyl vinyl ketone (**b**), is the crucial rate-limiting step of the reaction yielding a Michael addition product adduct species (**C**). Interestingly, the subsequent intramolecular rearrangement of (**C**) to a different O-bound intermediate (**D**) exhibit nearly equal activation barrier.

© 2014 Elsevier B.V. All rights reserved.

Introduction

Named after Arthur Michael [1], the conjugate addition of nucleophiles to acceptor activated olefin and alkyne substrates is now a much recognized strategy for an efficient and versatile construction of C–C bonds [2]. The reaction offers a large variety of the conjugate addition products from a broad scope of the Michael donor and Michael acceptor substrate bases. Depending upon the nature of the nucleophile, many of its variants, in the form of hetero-Michael reactions, whose recent examples include, the azo-Michael [3], sulpha-Michael [4], phospho-Michael [5] and oxo-Michael [6] have surfaced alongside. The classical Michael additions are typically base catalyzed that also promote many unwanted secondary reactions like aldol cyclization, ester solvolysis and etc, thus affecting the overall yield of the reaction. Towards this end, the transition metal mediated Michael additions [7], that allow the use of mild and neutral reaction conditions, offer attractive alternatives over the base catalyzed Michael additions. Despite the success with transition metals, the parallel development of organocatalytic version of the Michael addition [8] has also gained popularity in the

recent past primarily for its 'green' nature that avoids the use of metals, thereby providing a nontoxic, readily available and convenient method [9]. However, the organocatalysis too is often plagued by its own limitations like the requirement of high catalyst loadings, restricted reaction conditions and narrow substrate scope.

In this backdrop our specific goal is in developing new bifunctional catalysts for carrying out the Michael addition under base-free conditions. We rationalized that the bifunctional catalysts by virtue of the presence of two orthogonal functionalities in the form of an acidic and a basic site may promote dual activations of both of the reacting partners namely, a nucleophile and an electrophile, under mild conditions in a highly efficient manner [10,11]. For achieving the base-free Michael reaction, the built-in basicity of the basic site of the bifunctional catalyst should be comparable to that of an external base with regard to being able to generate the nucleophile for the conjugate addition by the deprotonation of an acidic hydrogen of one of the reactants (*i.e.* of a Michael donor). In this regard, the donor-functionalized *N*-heterocyclic carbene complexes of transition metals have attracted attention lately [12]. Hence, the conceptual realization of a successful bifunctional catalyst heavily relies on the cooperation between two reactions facilitated individually by two orthogonal effects that comprise of the generation of a carbanion by deprotonation of the Michael donor by the built-in basic site on the ligand along with the activation of the Michael acceptor by the

* Corresponding authors. Fax: +91 22 2572 3480.

E-mail addresses: rajaraman@chem.iitb.ac.in (G. Rajaraman), pghosh@chem.iitb.ac.in (P. Ghosh).

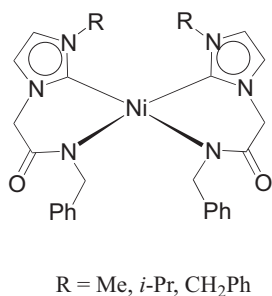


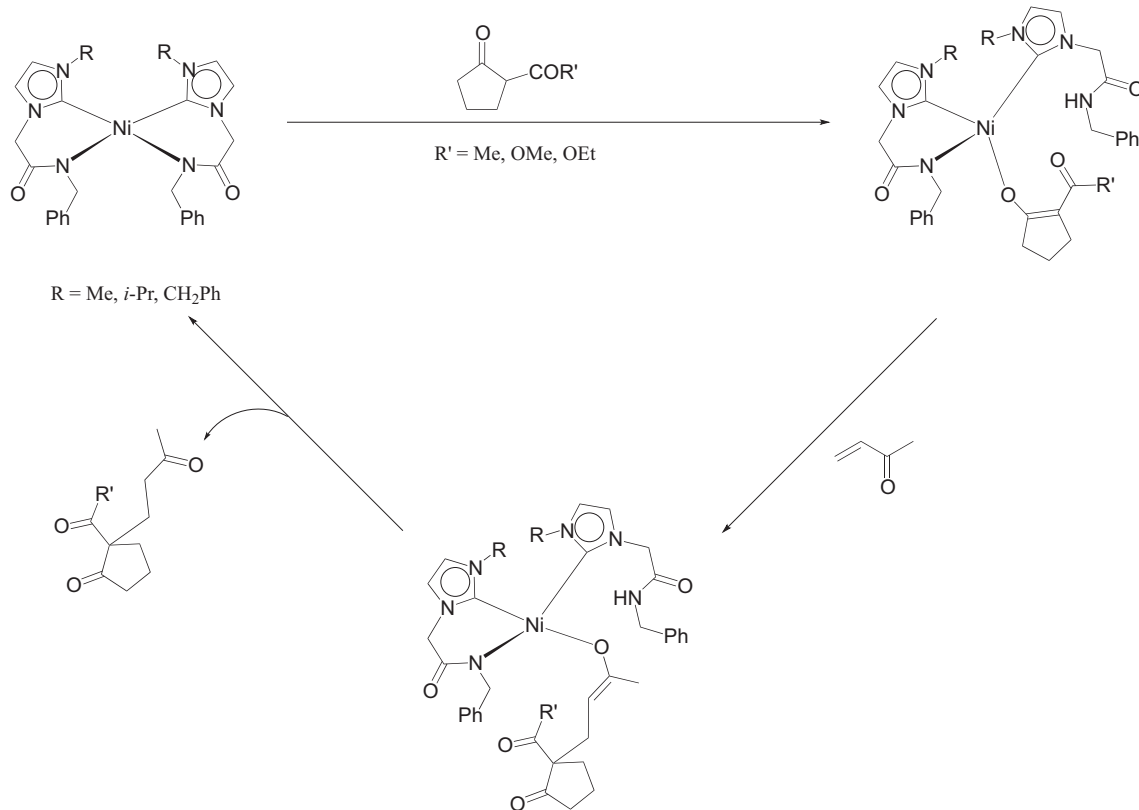
Fig. 1. Bifunctional Ni(II)-NHC catalysts used for the base-free Michael addition reaction (see Ref. [16]).

acidic metal site of the bifunctional catalyst through coordination to it. Building upon the above rationale, as a part of our long-standing interest in the chemistry of *N*-heterocyclic carbenes [13], and their related catalytic [14] and biomedical applications [15], we have recently reported a series of bifunctional nickel precatalysts of chelating amido-functionalized *N*-heterocyclic carbene ligands for the base-free Michael addition reaction in air at room temperature (Fig. 1 and Scheme 1) [16]. In this context it is noteworthy that though the *N*-heterocyclic carbenes have made a lasting impression in the field of transition metal mediated homogenous catalysis, the development of bifunctional catalysts using these ligands have surprisingly been rather limited, and in light of which our current effort assumes significance. In the absence of any prior mechanistic studies [17] of such base-free Michael addition reaction by any bifunctional transition metal catalysts of the *N*-heterocyclic carbene ligands, we set out to perform the same.

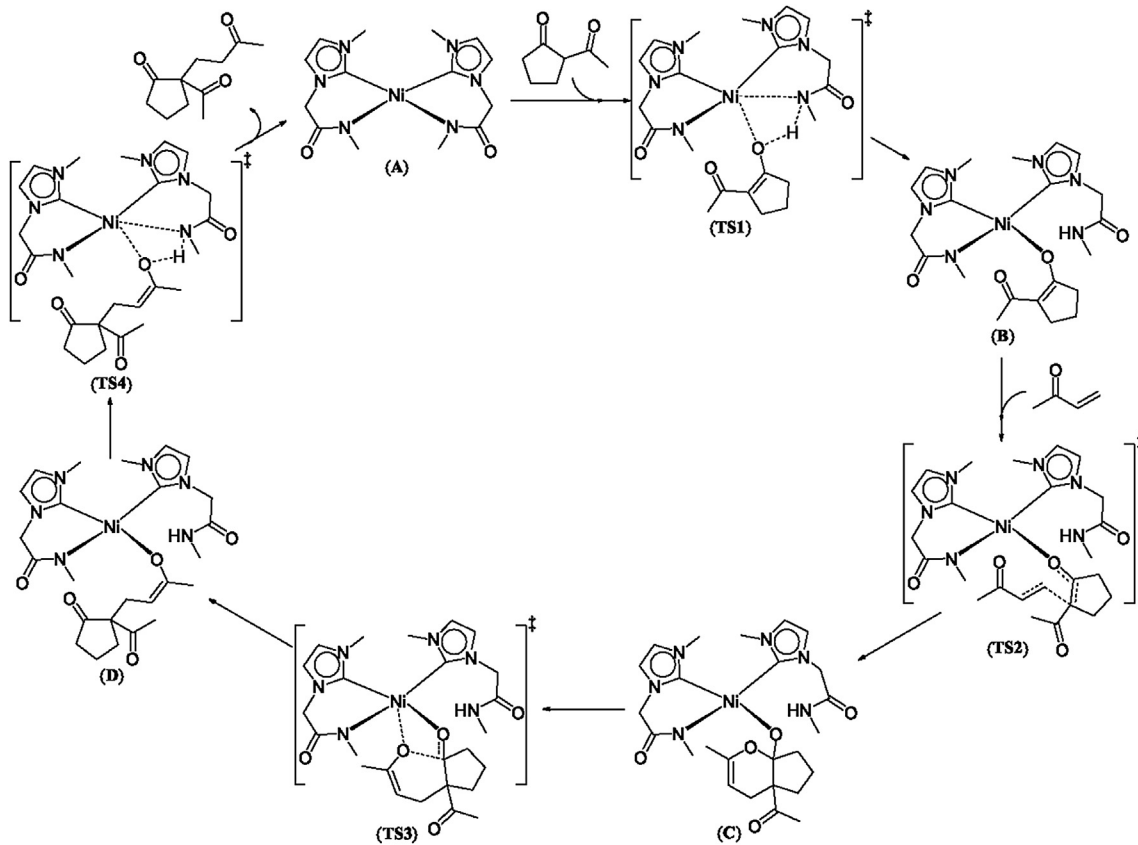
Herein, we report a computational investigation of the base-free Michael addition reaction of a β -dicarbonyl compound, 2-acetyl-cyclopentanone (**a**), with an activated α,β -unsaturated olefin substrate, methyl vinyl ketone (**b**), catalyzed by a bifunctional nickel precatalyst, $[\text{1-(Me)-3-}N\text{-(methylacetamido)imidazol-2-ylidene}]_2\text{Ni}$ (**A**), that is supported over a chelating amido-functionalized *N*-heterocyclic carbene ligand (Schemes 2 and 3). The study aims at understanding the explicit role of the rationally designed nickel based bifunctional catalyst in partaking the Michael addition reaction under base-free conditions.

Results and discussion

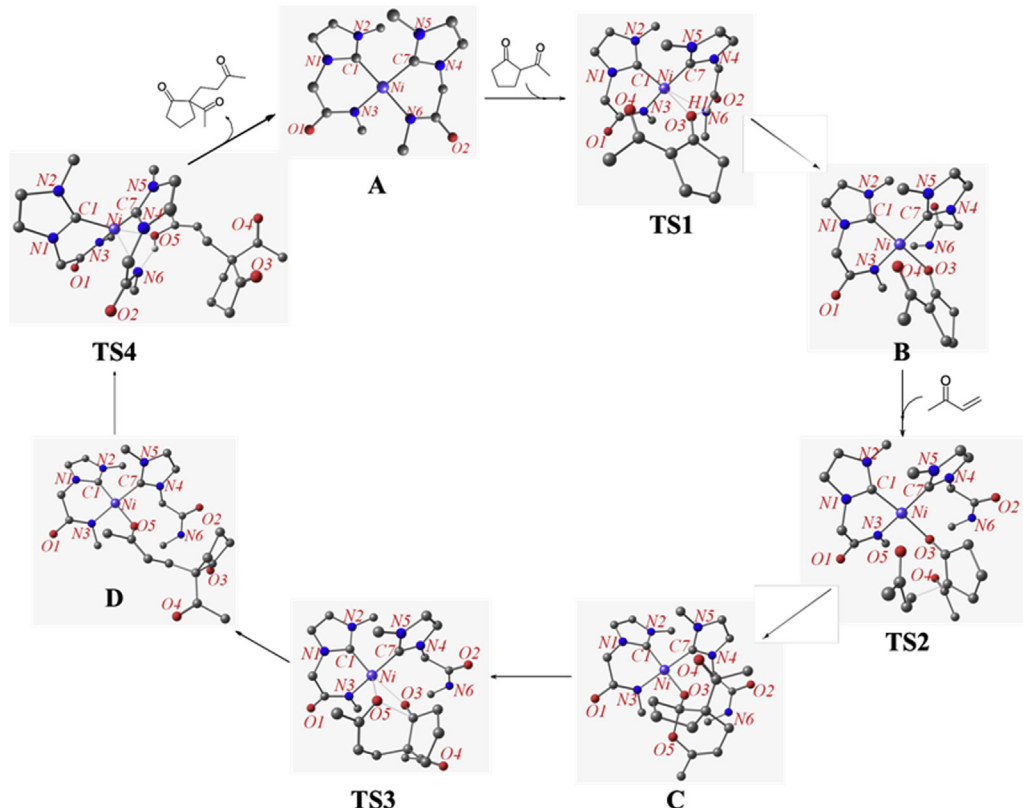
A proposed mechanism of a base-free Michael addition reaction of 1,3-dicarbonyl compounds with activated olefins mediated by a series of bifunctional nickel precatalysts under ambient conditions have been investigated in the current study [16] (Scheme 1). Towards this purpose a singlet spin-state mechanistic pathway was modeled employing density functional theory studies (Schemes 3 and Fig. 2). As for the computational simplicity, a methyl and an *N*-(methyl)acetamido moiety were chosen as the 1,3-substituents in a modified precatalyst (**A**) as opposed to the more elaborated ones of the nickel precatalysts (Fig. 1) reported earlier for the base-free Michael addition reaction under ambient conditions [16]. More specifically, a base-free Michael addition reaction between two representative substrates namely, 2-acetyl-cyclopentanone (**a**) and methyl vinyl ketone (**b**) as catalyzed by the simplified nickel precatalyst, $[\text{1-(Me)-3-}N\text{-(methylacetamido)imidazol-2-ylidene}]_2\text{Ni}$ (**A**) was thus chosen for the study. All of the stationary and transition states of proposed catalytic cycle were computed at B3LYP/LANL2DZ, 6-31G(d) level of theory by applying appropriate modification to the solid state structures of



Scheme 1. Proposed catalytic cycle for the base-free Michael addition reaction by Ni(II)-NHC complexes.



Scheme 2. Computed catalytic cycle for the base-free Michael addition reaction by a simplified Ni(II)-NHC complex (A).



Scheme 3. Computed catalytic cycle for base-free Michael addition reaction of 2-acetyl-cyclopentanone (**a**) with methyl vinyl ketone (**b**) as catalyzed by a representative bifunctional nickel N-heterocyclic carbene precatalyst (**A**).

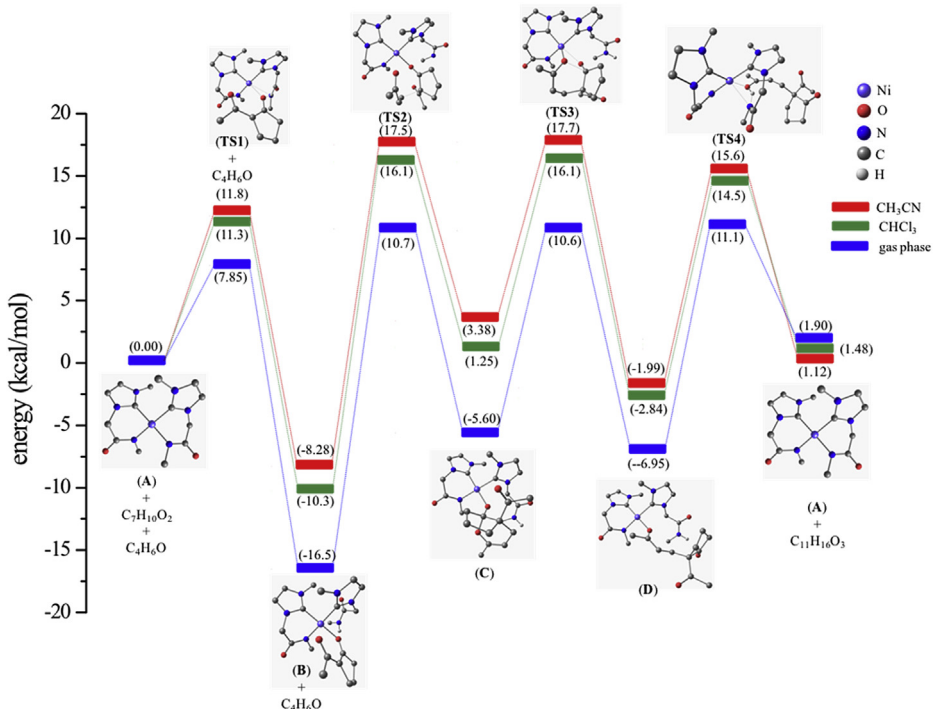


Fig. 2. An overlay of the computed isolated gas phase and solvent phase (MeCN and CHCl₃) total energy (*E*) with zero-point energy (ZPE) correction (*E* + ZPE) at B3LYP/LANL2DZ, 6-31G(d) level of theory for base-free Michael addition of 2-acetyl-cyclopentanone (**a**) with methyl vinyl ketone (**b**) as catalyzed by a representative bifunctional nickel N-heterocyclic carbene precatalyst (**A**).

the Michael precatalysts [16], whose coordinates were obtained from the X-ray analysis (Fig. 2–6 and Supporting information Figs. S4, S5, S7–S14 and Tables S1, S3–S13). Notably, with all of the molecular structures of the reported precatalysts [16]

exhibiting a *cis*-disposition of the two 1,3-disubstituted *N*-heterocyclic carbene ligands around the metal center, the simplified precatalyst (**A**) was so chosen of such *cis*-geometry (Supporting information Fig. S5). Indeed, a geometry depicting the *trans*-

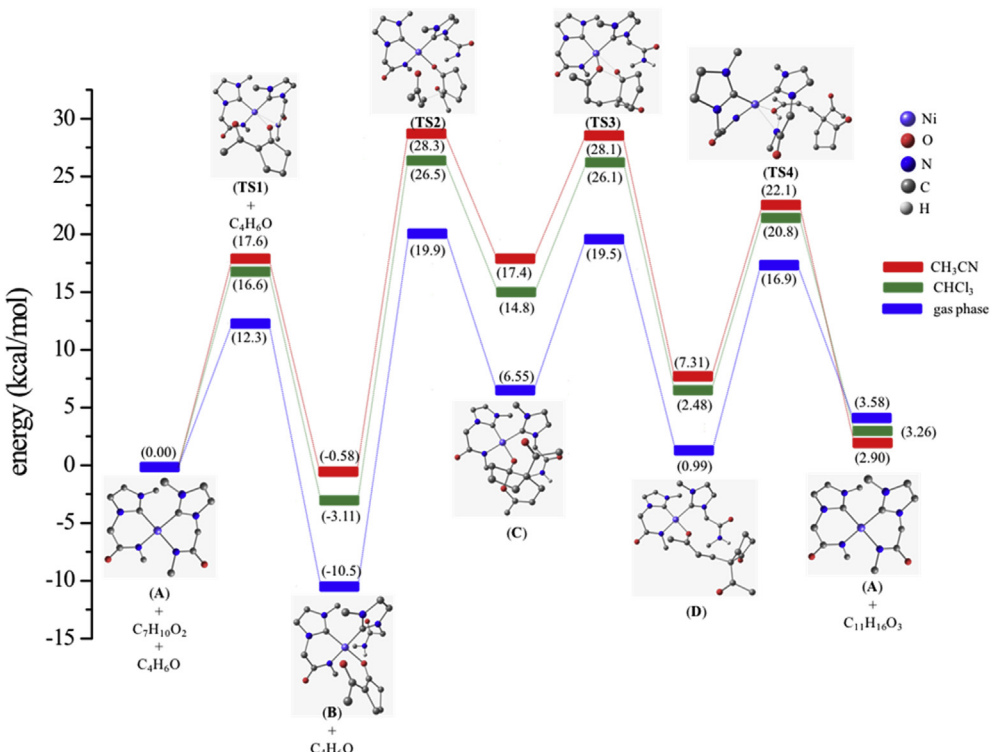


Fig. 3. An overlay of the computed isolated gas phase and solvent phase (MeCN and CHCl₃) total energy (*E*) with zero-point energy (ZPE) correction (*E* + ZPE) at B3LYP/LANL2DZ, TZVP level of theory for base-free Michael addition of 2-acetyl-cyclopentanone (**a**) with methyl vinyl ketone (**b**) as catalyzed by a representative bifunctional nickel N-heterocyclic carbene precatalyst (**A**).

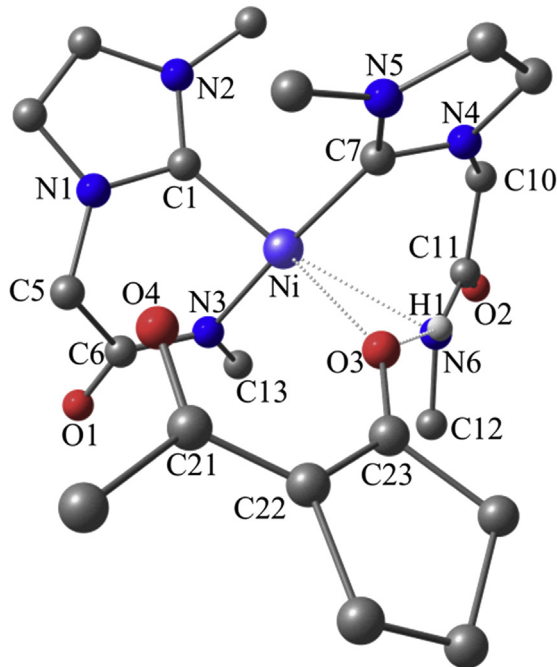


Fig. 4. Computed structure of *cis*-¹TS1. Selected bond lengths (\AA), bond angles ($^\circ$); Ni—C1 1.865, Ni—C7 1.939, Ni—N3 1.881, Ni—N6 2.661, N6···H1 1.039, O3···H1 1.723, Ni···O3 2.574, Ni···O4 3.701, C1—Ni—O3 134.16, C7—Ni—N3 176.23, C1—Ni—C7 95.85, C1—Ni—N3 87.80, C7—Ni—O3 72.08, N3—Ni—O3 105.94. Calculated imaginary frequency involving Ni···O3, O3···H1···N6 and N6···Ni bond is i87 cm^{-1} .

disposition of the two *N*-heterocyclic carbene ligands around the nickel center was found to be significantly higher in energy by 7.8 kcal/mol than that of the corresponding *cis* analog at the B3LYP/LANL2DZ, 6-31G(d) level of theory (Supporting Information Figs. S1–S2, S5–S6 and Tables S1 and S2). Additional single-point calculations were performed on the fully optimized geometries of the stationary points and the transition states by using a higher triple ξ -basis set at the B3LYP/LANL2DZ, TZVP and the B3LYP/TZVP levels of theory for further substantiation of the results (Figs. 2–6

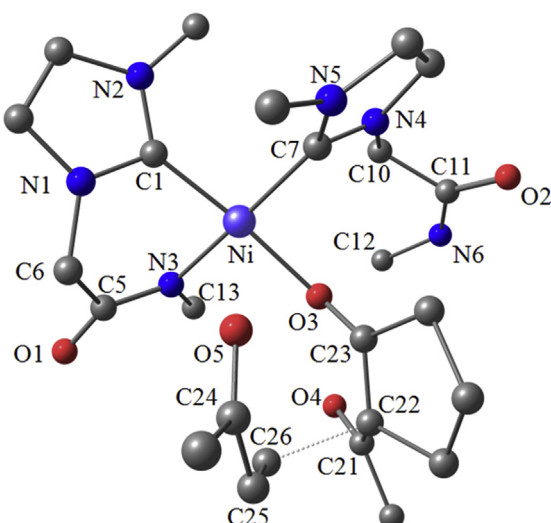


Fig. 5. Computed structure of *cis*-¹TS2. Selected bond lengths (\AA), bond angles ($^\circ$); Ni—C1 1.881, Ni—C7 1.930, Ni—N3 1.917, Ni—O3 1.997, Ni···O5 3.034, C22···C26 1.957, O3—C23 1.256, C23—C22 1.458, C1—Ni—O3 175.15, C7—Ni—N3 175.96, C1—Ni—C7 93.66, C1—Ni—N3 86.10, C7—Ni—O3 90.43, N3—Ni—O3 89.98. Calculated imaginary frequency involving C22···C26 bond is i318 cm^{-1} .

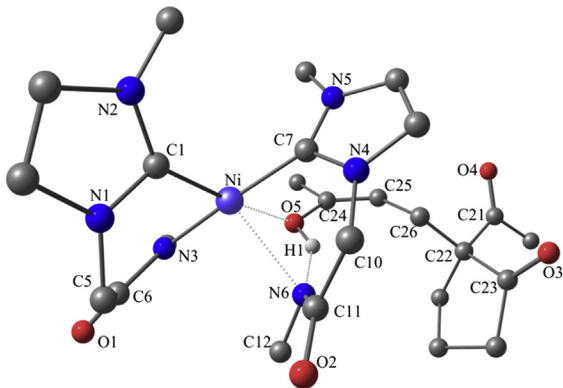


Fig. 6. Computed structure of *cis*-¹TS4. Selected bond lengths (\AA), bond angles ($^\circ$); Ni—C1 1.885, Ni—C7 1.930, Ni—N3 1.893, Ni···N6 2.457, N6···H1 1.646, O5···H1 1.025, Ni···O5 2.383, C1—Ni—O5 172.68, C7—Ni—N3 176.34, C1—Ni—C7 96.04, C1—Ni—N3 87.60, C7—Ni—O5 83.90, N3—Ni—O5 92.52. Calculated imaginary frequency involving O5···Ni, N6···Ni and N6···H1···O5 bonds is i106 cm^{-1} .

and Supporting information Figs. S3–S5, S8–S14 and Tables S1, S3–S13) and the results of which closely matched with each other. The solvent effects were incorporated via polarizable continuum model (PCM) calculations, done for the CH_3CN and CHCl_3 mediums. The values pertaining to the CHCl_3 medium, obtained at B3LYP/LANL2DZ, TZVP level of theory, are used in the current discussion. Both of the total energy (E) with zero-point energy (ZPE) correction ($E + \text{ZPE}$) and the free energy (ΔG) profiles were obtained for a better understanding of the chemical reaction space of the base-free Michael addition reaction between the representative β -dicarbonyl compound, 2-acetyl-cyclopentanone (**a**), and the representative α,β -unsaturated carbonyl compound, methyl vinyl ketone (**b**), as catalyzed by a representative simplified bifunctional nickel *N*-heterocyclic carbene precatalyst of the type (**A**) (Figs. 2 and 3 and Supporting information Figs. S2–S4). Throughout the text the energy values pertaining to the total energy (E) with zero-point energy (ZPE) correction ($E + \text{ZPE}$) profile have been used owing to the overestimation of the entropy term observed in the corresponding free energy profile [18].

In keeping with the earlier observed diamagnetic nature of the nickel precatalysts [16], an initiating species having a singlet spin-state, *cis*-¹A, was thus chosen for the computational modeling studies. The square planar structure of *cis*-¹A exhibited slightly lower Ni—C_{carbene} distances [$d/(Ni—C1) = 1.914 \text{ \AA}$ and $d/(Ni—C7) = 1.915 \text{ \AA}$] than the sum of the respective covalent radii of Ni and C ($\text{Ni—C} = 1.926 \text{ \AA}$) [22] while the Ni—N_{amide} distances [$d/(Ni—N3) = 1.939 \text{ \AA}$ and $d/(Ni—N6) = 1.938 \text{ \AA}$] were slightly higher than the similar sum of the covalent radii of Ni and N ($\text{Ni—N} = 1.854 \text{ \AA}$) [19]. As expected, all of the angles at the nickel center conformed to an ideal value of 90° (Supporting information Fig. S5 and Table S1). The NBO analysis revealed the polar nature of the Ni—C1 (carbene) and Ni—C7 (carbene) bonds with predominantly higher percentages of electron contribution coming from C1 (78.7) and C7 (78.7) and considerably lower percentages of electron contribution from Ni (21.2) in each. Similarly, the Ni—N3 (amide) and Ni—N6 (amide) bonds exhibited even higher percentages of electron contribution arising from N3 (84.3) and N6 (84.3) and much lower percentages of electron contribution from Ni (15.6) in each (Supporting information Table S14).

The catalytic cycle proceeds with the coordination of the substrate, 2-acetyl-cyclopentanone (**a**), to the precatalyst (**A**) yielding the corresponding 1,3-dicarbonyl adduct species (**B**) via a transition state **TS1** that exhibits a barrier of 16.6 kcal/mol. The binding of the 1,3-dicarbonyl substrate, 2-acetyl-cyclopentanone (**a**), to the metal

center occurs through its enol-form, as opposed to the keto-form, as the former is more favorable to donate the hydrogen atom to the amido-N of the functionalized sidearm [8b].

The transition state **TS1** has been characterized by an imaginary frequency of $i87\text{ cm}^{-1}$ exhibiting displacement vectors along the $\text{Ni}\cdots\text{O}_3$, $\text{Ni}\cdots\text{N}_6$, $\text{O}_3\cdots\text{H}_1$ and $\text{N}_6\cdots\text{H}_1$ interactions. The ring carbonyl O_3 of the substrate (**a**) was seen interacting with $\text{N}-\text{H}$ (H_1) proton of the protonated non-chelated amido sidearm substituents. The $\text{Ni}\cdots\text{O}_3$ distance of 2.574 \AA was significantly lower than the sum of the individual van der Waals radii of Ni and O ($\text{Ni}\cdots\text{O} = 2.95\text{ \AA}$) [20] and is indicative of a strong interaction. On the contrary, the observed oxygen $\text{O}_3\cdots\text{H}_1$ distance of 1.723 \AA when compared to the sum of the individual van der Waals radii of O and H ($\text{O}\cdots\text{H} = 1.72\text{ \AA}$) [20] suggested a relatively weaker interaction. It is interesting to note that the amido-sidearm of one of the *N*-heterocyclic carbene ligand in **A** was protonated by the active hydrogen atom of the 1,3-dicarbonyl substrate, 2-acetyl-cyclopentanone (**a**), and which subsequently got dechelated from the nickel center in the transition state **TS1** (Fig. 4 and Supporting Information Table S3). Quite unexpectedly, the NBO analysis reveals that the dechelation of amido- N_6 sidearm from the nickel center [$d/(\text{Ni}-\text{C}_7) = 1.939\text{ \AA}$] in the **TS1** leads to an increase in the natural charge (0.437) at nickel in the **TS1** relative to that in **A** (+0.307) and as a consequence of which, shorter $\text{Ni}-\text{C}_{\text{carbene}}$ [$d/(\text{Ni}-\text{C}_1) = 1.865\text{ \AA}$ and $d/(\text{Ni}-\text{C}_7) = 1.939\text{ \AA}$] and $\text{Ni}-\text{N}_{\text{amido}}$ [$d/(\text{Ni}-\text{N}_3) = 1.881\text{ \AA}$] distances were observed as compared to that in the initiating species **A** [$d/(\text{Ni}-\text{C}_1) = 1914\text{ \AA}$ and $d/(\text{Ni}-\text{C}_7) = 1.915\text{ \AA}$] and $\text{Ni}-\text{N}_{\text{amido}}$ [$d/(\text{Ni}-\text{N}_3) = 1.939\text{ \AA}$]. The acetyl oxygen O_4 was found to be deposited away from the metal center ($\text{Ni}\cdots\text{O}_4 = 3.701\text{ \AA}$) (Supporting information Table S14).

Transition state **TS1** results in a lower energy (-3.11 kcal/mol) square planar intermediate (**B**) having one amido functionalized *N*-heterocyclic carbene ligand chelated to the metal center through the carbene carbon C_1 and the amido nitrogen N_3 atom while the other *N*-heterocyclic carbene ligand, possessing the protonated amide moiety, was bound to the nickel center through the carbene carbon C_7 only. The fourth site was occupied by the ring carbonyl oxygen O_3 atom that exhibited a strong $\text{Ni}-\text{O}_3$ interaction as seen from a significantly shorter $\text{Ni}-\text{O}_3$ distance of 1.960 \AA relative to that in the transition state **TS1** [$d/(\text{Ni}\cdots\text{O}_3) = 2.574\text{ \AA}$]. The NBO analysis reveals that the coordination of the ring carbonyl oxygen O_3 atom to the nickel center resulted in accumulation of the electron density at the metal center as seen from the natural charge of +0.366 at the nickel in **B** diminishing from the corresponding value of +0.437 at the metal in **TS1** (Supporting information Table S14). An interesting fallout of the shorter $\text{Ni}-\text{O}_3$ distance (1.960 \AA), is the elongation of the remaining three bonds to the nickel center in **B**, *i.e.* of the $\text{Ni}-\text{C}_{\text{carbene}}$ [$d/(\text{Ni}-\text{C}_1) = 1.899\text{ \AA}$ and $d/(\text{Ni}-\text{C}_7) = 1.955\text{ \AA}$] and the $\text{Ni}-\text{N}_{\text{amido}}$ [$d/(\text{Ni}-\text{N}_3) = 1.946\text{ \AA}$] distances in comparison to the corresponding ones in the transition state **TS1** [$d/(\text{Ni}-\text{C}_1) = 1.865\text{ \AA}$, $d/(\text{Ni}-\text{C}_7) = 1.939\text{ \AA}$ and $d/(\text{Ni}-\text{N}_3) = 1.881\text{ \AA}$] (Supporting information Fig. S7 and Table S4).

The reaction proceeds by the approach of the methyl vinyl ketone (**b**) substrate to the Ni bound acetyl-cyclopentenolate moiety, whose ring carbon C_{22} attacks the activated olefinic-end carbon C_{26} of the methyl vinyl ketone (**b**) substrate exhibiting a characteristic imaginary frequency of $i312\text{ cm}^{-1}$ along the $\text{C}_{22}\cdots\text{C}_{26}$ bond formation in the transition state **TS2** and which marks an uphill barrier of 29.6 kcal/mol from the nearest reacting species **B**. Incidentally, this step represents the rate-determining step of the overall reaction. This is expected as the C–C bond formation is taking place at this transition state and the HOMO of the **TS2** reveals that essentially the π -electrons of both the methyl vinyl ketone moiety and the Ni bound acetyl-cyclopentenolate moiety participate in this transition state (Supporting information

Fig. S15). Of particular interest is the $\text{C}_{22}\cdots\text{C}_{26}$ distance of 1.957 \AA that is longer than a C–C single bond distance (1.544 \AA) [19] but shorter than twice the van der Waals radii of C (3.06 \AA) [20]. As expected, the $\text{O}_3\cdots\text{C}_{23}$ distance (1.256 \AA) has shortened slightly in the transition state **TS2** as compared to the same in **B** (1.288 \AA) and is consistent with one having a partial double bond character. Lastly, the $\text{C}_{23}\cdots\text{C}_{22}$ distance of 1.458 \AA in transition state **TS2** is longer than the corresponding distance in **B** (1.394 \AA) (Fig. 5 and Supporting information Table S5).

The transition state **TS2** results in a stable square planar intermediate **C**, in which the Michael addition product was found bound to the metal center, and whose formation was endergonic by 17.9 kcal/mol with respect to the nearest reacting species **B**. As expected, the $\text{Ni}-\text{C}_{\text{carbene}}$ bond distances [$d/(\text{Ni}-\text{C}_1) = 1.907\text{ \AA}$ and $d/(\text{Ni}-\text{C}_7) = 1.931\text{ \AA}$] and the $\text{Ni}-\text{N}_{\text{amido}}$ distance [$d/(\text{Ni}-\text{N}_3) = 1.931\text{ \AA}$] conform to the respective $\text{Ni}-\text{C}$ (1.926 \AA) and $\text{Ni}-\text{N}$ (1.854 \AA) [19] single bond lengths. Another important structural aspect of the intermediate **C** is about the presence of a six-membered ring that arise out of an intramolecular attack of the nucleophilic oxygen O_5 atom on to the electrophilic carbon C_{23} atom within the nickel bound Michael addition product moiety and which exhibits a $\text{O}_5\cdots\text{C}_{23}$ distance of 1.498 \AA consistent with a $\text{O}-\text{C}$ single bond length (1.432 \AA) [19] (Supporting information Fig. S8 and Table S6). Also complying with the nucleophilic attack of O_5 atom on to the C_{23} atom, the natural charge on O_5 atom decreased to -0.580 from that of O_5 atom (-0.732) in the methyl vinyl ketone (**d**) substrate (Supporting information Table S14).

The intermediate **C** further undergoes a rearrangement *via* a transition state **TS3** displaying a barrier height of 11.3 kcal/mol from its nearest reactant species **C** to give an intermediate **D** that is more stabilized by -11.3 kcal/mol with respect to **C**. In the transition state **TS3**, the rearrangement proceeds *via* the formation of a $\text{Ni}\cdots\text{O}_5$ bond (2.256 \AA) concomitant with the cleavages of $\text{Ni}\cdots\text{O}_3$ (2.400 \AA) and $\text{O}_5\cdots\text{C}_{23}$ (2.314 \AA) bonds. The transition state **TS3** has been characterized by an imaginary frequency of $i105\text{ cm}^{-1}$ depicting displacement vectors in the direction of $\text{Ni}\cdots\text{O}_5$ bond formation and of the $\text{Ni}\cdots\text{O}_3$ and $\text{O}_5\cdots\text{C}_{23}$ bond cleavages (Supporting information Fig. S9 and Table S7).

The intermediate **D** is also of a square planar geometry, similar to that of the intermediate **C**, but differing by the binding of the Michael addition product moiety to the metal center *via* the O_5 oxygen atom as opposed to the O_3 atom in the intermediate **C**. The $\text{Ni}\cdots\text{O}_5$ bond distance of 1.903 \AA in the intermediate **D** is slightly smaller than the $\text{Ni}\cdots\text{O}_3$ bond distance of 1.932 \AA observed in the intermediate **C** (Supporting information Fig. S10 and Table S8).

The final step of the mechanistic cycle involves an intramolecular rebound proton transfer in the transition state **TS4** between the amido N_6 atom and the oxygen O_5 atom of the nickel bound enolate of the Michael addition product moiety along with the cleavage of the $\text{Ni}\cdots\text{O}_5$ bond. The transition state **TS4** exhibits a barrier of 17.3 kcal/mol with respect to the nearest reactant species **D** as characterized by an imaginary frequency of $i106\text{ cm}^{-1}$ that display displacement vectors along the direction of $\text{Ni}\cdots\text{N}_6$ bond formation and $\text{Ni}\cdots\text{O}_5$ bond cleavage (Fig. 6 and Supporting information Table S9). The transition state **TS4** finally yields the initiating catalytic species **A** along with the enol form of the Michael addition product, that further gets stabilized by 11.8 kcal/mol in its lower energy keto form (Supporting information Figs. S13–S14, S16–S17 and Tables S12 and S13).

Overall, the Michael addition reaction of 2-acetyl-cyclopentanone (**a**) with methyl vinyl ketone (**b**) as catalyzed by a bifunctional nickel precatalyst (**A**) is slightly endergonic by 3.26 kcal/mol . The attack of the methyl vinyl ketone (**b**) substrate on to the 2-acetyl-cyclopentenolate moiety bound to the nickel center in the intermediate **B** yielding the species **C** marks the rate-

determining step of the overall Michael addition reaction. Notably, the subsequent rearrangement step from the species C to D was found to be almost equally competitive displaying only a marginally lower activation barrier.

Conclusions

In summary, a base-free Michael addition reaction of 2-acetyl-cyclopentanone (**a**) and methyl vinyl ketone (**b**), as catalyzed by a bifunctional nickel N-heterocyclic carbene complex, [1-(Me)-3-N-(methylacetamido)imidazol-2-ylidene]₂Ni (**A**), has been investigated using density functional theory (DFT) studies. The catalytic cycle initiates with the binding of 2-acetyl-cyclopentanone (**a**) to the nickel precatalyst (**A**) as a result of the deprotonation of an acidic C–H bond of 2-acetyl-cyclopentanone (**a**) by an amido ligand sidearm of the nickel precatalyst (**A**) to give an intermediate (**B**). A nucleophilic attack of the carbanion of the metal bound enolate moiety of the 1,3-dicarbonyl adduct species (**B**) on to an activated olefinic substrate namely, methyl vinyl ketone (**b**), yields the much desired Michael addition product adduct species (**C**) that further undergo intramolecular rearrangement to an intermediate (**D**). Subsequently, an intramolecular protonation of the metal bound Michael addition product species by an amido ligand sidearm of **D** yields the corresponding Michael addition product along with the regeneration of the starting catalytic species (**A**).

Experimental section

Computational methods

Density functional theory (DFT) calculations were performed on the reactant, product, transition states and the intermediates using GAUSSIAN 09 [21] suite of quantum chemical programs. In particular, the DFT calculations were performed on the stationary (**A–D**) and the transition states (**TS1–TS4**) of the proposed mechanistic cycle (Scheme 2). The Becke three parameter exchange functional in conjunction with Lee–Yang–Parr correlation functional (B3LYP) has been employed in the study [22]. The polarized basis set 6-31G(d) [23] was used to describe oxygen, carbon, nitrogen and hydrogen atoms while the LANL2DZ basis set was used for the nickel atom [24]. Finally, higher level single-point calculations on the stationary (**A–D**) and the transition states (**TS1–TS4**) of the proposed mechanistic cycle (Schemes 2 and 3) were performed on the respective B3LYP/LANL2DZ, 6-31G(d) optimized geometries using LANL2DZ basis set for Ni atom and TZVP basis set for all other atoms [25]. Natural bond orbital (NBO) analysis [26] was performed using NBO 3.1 program implemented in the GAUSSIAN 09 package. The transition state (TS) optimization method based on the Berny algorithm was used for the transition state optimizations [27]. Frequency calculations were performed for all of the optimized structures to characterize the stationary points as minima and the transition states as maxima. The solvation energy has been incorporated using Polarizable Continuum Model (PCM) [28] with CHCl₃ and CH₃CN solvents via single-point energy calculations of the optimized gas phase geometries. All the energetics of the potential energy surfaces discussed are that of the solvation electronic energy values in CHCl₃ unless otherwise stated.

Acknowledgments

We thank Department of Science and Technology, (Grant No: SR/S1/IC-15/2011), New Delhi, for financial support of this research. Computational facilities from the IIT Bombay Computer Center are gratefully acknowledged. MK thanks BRNS, Mumbai for research fellowship.

Appendix A. Supplementary data

Supplementary data related to this article can be found at <http://dx.doi.org/10.1016/j.jorgchem.2014.02.012>.

References

- [1] (a) T. Tokoroyama, Eur. J. Org. Chem. (2010) 2009–2016;
(b) T. Poon, B.P. Mundy, T.W. Shattuck, J. Chem. Educ. 79 (2002) 264–267;
(c) A.B. Costa, J. Chem. Educ. 48 (1971) 243–246.
- [2] (a) C.F. Nisinga, S. Bräse, Chem. Soc. Rev. 41 (2012) 988–999;
(b) A.G. Csaky, G.D.L. Herrana, M.C. Murcia, Chem. Soc. Rev. 39 (2010) 4080–4102;
(c) C.F. Nisinga, S. Bräse, Chem. Soc. Rev. 37 (2008) 1218–1228.
- [3] (a) S.-J. Lee, S.-H. Youn, C.-W. Cho, Org. Biomol. Chem. 9 (2011) 7734–7741;
(b) D.L. Priebbenow, S.G. Stewart, F.M. Pfeffer, Org. Biomol. Chem. 9 (2011) 1508–1515;
(c) Y. Ying, H. Kim, J. Hong, Org. Lett. 13 (2011) 796–799;
(d) Q. Gu, S.-L. You, Chem. Sci. 2 (2011) 1519–1522;
(e) U. Uria, J.L. Vicario, D. Badia, L. Carrillo, Chem. Commun. (2007) 2509–2511.
- [4] (a) N.K. Rana, R. Unhale, V.K. Singh, Tetrahedron Lett. 53 (2012) 2121–2124;
(b) W. Yang, D.-M. Du, Org. Biomol. Chem. 10 (2012) 6876–6884;
(c) X.-F. Wang, Q.-L. Hua, Y. Cheng, X.-L. An, Q.-Q. Yang, J.-R. Chen, W.-J. Xiao, Angew. Chem. Int. Ed. 49 (2010) 8379–8383.
- [5] (a) B. Cho, C.-H. Tan, M.W. Wong, Org. Biomol. Chem. 9 (2011) 4550–4557;
(b) X. Luo, Z. Zhou, X. Li, X. Liang, J. Ye, RSC Adv. 1 (2011) 698–705;
(c) S. Wen, P. Li, H. Wu, F. Yu, X. Liang, J. Ye, Chem. Commun. 46 (2010) 4806–4808;
(d) D. Enders, A. Saint-Dizier, M.-I. Lannou, A. Lenzen, Eur. J. Org. Chem. (2006) 29–49;
(e) L. Tedeschi, D. Enders, Org. Lett. 3 (2001) 3515–3517.
- [6] (a) P.A. Evans, A. Grisin, M.J. Lawler, J. Am. Chem. Soc. 134 (2012) 2856–2859;
(b) J.-H. Xie, L.-C. Guo, X.-H. Yang, L.-X. Wang, Q.-L. Zhou, Org. Lett. 14 (2012) 4758–4761;
(c) P.A. Hume, J. Sperry, M.A. Brimble, Org. Biomol. Chem. 9 (2011) 5423–5430;
(d) R.B. Devi, M. Henrot, M.D. Paolis, J. Maddaluno, Org. Biomol. Chem. 9 (2011) 6509–6512;
(e) L. Zu, S. Zhang, H. Xie, W. Wang, Org. Lett. 11 (2009) 1627–1630.
- [7] (a) D.C. Schmitt, E.J. Malow, J.S. Johnson, J. Org. Chem. 77 (2012) 3246–3251;
(b) L. Liu, R. Sarkisian, Z. Xu, H. Wang, J. Org. Chem. 77 (2012) 7693–7699;
(c) C. Fallon, H.W. Lam, Chem. Eur. J. 18 (2012) 11214–11218;
(d) C. Zhao, F.D. Toste, R.G. Bergman, J. Am. Chem. Soc. 133 (2011) 10787–10789;
(e) Z. Dong, J. Feng, W. Cao, X. Liu, L. Lin, X. Feng, Tetrahedron Lett. 52 (2011) 3433–3436;
(f) V. Rajalakshmi, V.R. Vijayaraghavan, B. Varghese, A. Raghavan, Inorg. Chem. 47 (2008) 5821–5830.
- [8] (a) N. Molletti, N.K. Rana, V.K. Singh, Org. Lett. 14 (2012) 4322–4325;
(b) S. Deuri, P. Phukan, Int. J. Quant. Chem. 112 (2012) 801–808;
(c) K. Asano, S. Matsubara, J. Am. Chem. Soc. 133 (2011) 16711–16713;
(d) X. Cao, G. Wang, R. Zhang, Y. Wei, W. Wang, H. Sun, L. Chen, Org. Biomol. Chem. 9 (2011) 6487–6490;
(e) Z. Zheng, B.L. Perkins, B. Ni, J. Am. Chem. Soc. 132 (2010) 50–51.
- [9] (a) F. Giacalone, M. Gruttaduria, P. Agrigento, R. Noto, Chem. Soc. Rev. 41 (2012) 2406–2447;
(b) P.H.Y. Cheong, C.Y. Legault, J.M. Um, N. Celebi-Olcum, K.N. Houk, Chem. Rev. 111 (2011) 5042–5137;
(c) A.N.R. Alba, X. Companyo, R. Rios, Chem. Soc. Rev. 39 (2010) 2018–2033;
(d) S. Bertelsen, K.A. Jorgensen, Chem. Soc. Rev. 38 (2009) 2178–2189;
(e) Z. Shao, H. Zhang, Chem. Soc. Rev. 38 (2009) 2745–2755;
(f) C. Palomo, M. Oiarbide, R. Lopez, Chem. Soc. Rev. 38 (2009) 632–653;
(g) B. List, Chem. Rev. 107 (2007) 5413–5415;
(h) D. Enders, O. Niemeier, A. Henseler, Chem. Rev. 107 (2007) 5606–5655.
- [10] (a) C. Wetzel, P.C. Kunz, I. Thiel, B. Spangler, Inorg. Chem. 50 (2011) 7863–7870;
(b) T. Ikariya, Top. Organomet. Chem. 37 (2011) 31–53;
(c) K. Lang, J. Park, S. Hong, J. Org. Chem. 75 (2010) 6424–6435;
(d) Y. Liu, B. Sun, B. Wang, M. Wakem, L. Deng, J. Am. Chem. Soc. 131 (2009) 418–419;
(e) M. Shibasaki, M. Kanai, K. Funabashi, Chem. Commun. (2002) 1989–1999.
- [11] (a) D.H. Paull, C.J. Abraham, M.T. Scerba, E.A. Iden-Danforth, T. Lectka, Acc. Chem. Res. 41 (2008) 655–663;
(b) T. Ikariya, A.J. Blacker, Acc. Chem. Res. 40 (2007) 1300–1308.
- [12] (a) W.W.N. O, A.J. Lough, R.H. Morris, Organometallics 31 (2012) 2152–2165;
(b) H. Ohara, W.W.N. O, A.J. Lough, R.H. Morris, Dalton Trans. 41 (2012) 8797–8808;
(c) W.B. Cross, C.G. Daly, R.L. Ackerman, I.R. George, K. Singh, Dalton Trans. 40 (2011) 495–505;
(d) S. Kuwata, T. Ikariya, Chem. Eur. J. 17 (2011) 3542–3556;
(e) Y. Lee, B. Li, A.H. Hoveyda, J. Am. Chem. Soc. 131 (2009) 11625–11633.

- [13] (a) A. Kumar, P. Ghosh, *Eur. J. Inorg. Chem.* (2012) 3955–3969;
 (b) P. Ghosh, *J. Indian Inst. Sci.* 91 (2011) 521–533;
 (c) A. John, P. Ghosh, *Dalton Trans.* 39 (2010) 7183–7206.
- [14] (a) M. Katari, M.N. Rao, G. Rajaraman, P. Ghosh, *Inorg. Chem.* 51 (2012) 5593–5604;
 (b) R. Stephen, R.B. Sunoj, P. Ghosh, *Dalton Trans.* 40 (2011) 10156–10161;
 (c) M.K. Samantray, C. Dash, M.M. Shaikh, K. Pang, R.J. Butcher, P. Ghosh, *Inorg. Chem.* 50 (2011) 1840–1848;
 (d) C. Dash, M.M. Shaikh, R.J. Butcher, P. Ghosh, *Inorg. Chem.* 49 (2010) 4972–4983;
 (e) C. Dash, M.M. Shaikh, R.J. Butcher, P. Ghosh, *Dalton Trans.* 39 (2010) 2515–2524;
 (f) A. John, M.M. Shaikh, P. Ghosh, *Dalton Trans.* (2009) 10581–10591;
 (g) L. Ray, V. Katiyar, S. Barman, M.J. Raihan, H. Nanavati, M.M. Shaikh, P. Ghosh, *J. Organomet. Chem.* 692 (2007) 4259–4269;
 (h) L. Ray, M.M. Shaikh, P. Ghosh, *Organometallics* 26 (2007) 958–964.
- [15] (a) S. Ray, J. Asthana, J.M. Tanski, M.M. Shaikh, D. Panda, P. Ghosh, *J. Organomet. Chem.* 694 (2009) 2328–2335;
 (b) S. Ray, R. Mohan, J.K. Singh, M.K. Samantaray, M.M. Shaikh, D. Panda, P. Ghosh, *J. Am. Chem. Soc.* 129 (2007) 15042–15053.
- [16] (a) S. Kumar, A. Narayanan, M.N. Rao, M.M. Shaikh, P. Ghosh, *J. Organomet. Chem.* 696 (2012) 4159–4165;
 (b) S. Ray, M.M. Shaikh, P. Ghosh, *Eur. J. Inorg. Chem.* (2009) 1932–1941;
 (c) M.K. Samantaray, M.M. Shaikh, P. Ghosh, *Organometallics* 28 (2009) 2267–2275.
- [17] For a few isolated reports of theoretical studies on the conjugate Michael addition reactions catalyzed by *s*-, *p*- and *d*-block elements see: (a) Z. Su, H.W. Lee, C.K. Kim, *Org. Biomol. Chem.* 9 (2011) 6402–6409;
 (b) E.E. Kwan, D.A. Evans, *Org. Lett.* 12 (2010) 5124–5127;
 (c) J. Borowka, C. van Wüllen, *J. Organomet. Chem.* 691 (2006) 4474–4479.
- [18] (a) A. Ciancetta, C. Coletti, A. Marrone, N. Re, *Dalton Trans.* 41 (2012) 12960–12969;
 (b) X. Zhang, Z. Xib, *Phys. Chem. Chem. Phys.* 13 (2011) 3997–4004;
 (c) D.H. Wertz, *J. Am. Chem. Soc.* 102 (1980) 5316–5322.
- [19] L. Pauling, *The Nature of the Chemical Bond*, third ed., Cornell University Press, Ithaca, NY, 1960, pp. 224–256.
- [20] A. Bondi, *J. Phys. Chem.* 68 (1964) 441–451.
- [21] M.J. Frisch, G.W. Trucks, H.B. Schlegel, G.E. Scuseria, M.A. Robb, J.R. Cheeseman, G. Scalmani, V. Barone, B. Mennucci, G.A. Petersson, H. Nakatsuji, M. Caricato, X. Li, H.P. Hratchian, A.F. Izmaylov, J. Bloino, G. Zheng, J.L. Sonnenberg, M. Hada, M. Ehara, K. Toyota, R. Fukuda, J. Hasegawa, M. Ishida, T. Nakajima, Y. Honda, O. Kitao, H. Nakai, T. Vreven, J.A. Montgomery, J.E. Peralta, F. Ogliaro, M. Bearpark, J.J. Heyd, E. Brothers, K.N. Kudin, V.N. Staroverov, R. Kobayashi, J. Normand, K. Raghavachari, A. Rendell, J.C. Burant, S.S. Iyengar, J. Tomasi, M. Cossi, N. Rega, J.M. Millam, M. Klene, J.E. Knox, J.B. Cross, V. Bakken, C. Adamo, J. Jaramillo, R. Gomperts, R.E. Stratmann, O. Yazyev, A.J. Austin, R. Cammi, C. Pomelli, J.W. Ochterski, R.L. Martin, K. Morokuma, V.G. Zakrzewski, G.A. Voth, P. Salvador, J.J. Dannenberg, S. Dapprich, A.D. Daniels, O. Farkas, J.B. Foresman, J.V. Ortiz, J. Cioslowski, D.J. Fox, Gaussian 09, Revision A.1, Gaussian, Inc., Wallingford CT, 2009.
- [22] (a) A.D. Becke, *Phys. Rev. A* 38 (1988) 3098–3100;
 (b) C. Lee, W. Yang, R.G. Parr, *Phys. Rev. B* 37 (1988) 785–798.
- [23] (a) W.J. Hehre, R. Ditchfield, J.A. Pople, *J. Chem. Phys.* 56 (1972) 2257–2261;
 (b) G.A. Petersson, A. Bennet, T.G. Tensfeldt, M.A. Al-Laham, W.A. Shirley, J. Mantzaris, *J. Chem. Phys.* 89 (1988) 2193–2218;
 (c) G.A. Petersson, M.A. Al-Laham, *J. Chem. Phys.* 94 (1991) 6081–6090.
- [24] (a) G.I. Cardenas-Jiron, C. Gonzalez, J. Benavides, *J. Phys. Chem. C* 116 (2012) 16979–16984;
 (b) O. Gutierrez, D.J. Tantillo, *Organometallics* 29 (2010) 3541–3545;
 (c) M. Ishida, Y. Naruta, F. Tani, *Dalton Trans.* 39 (2010) 2651–2659;
 (d) O. Das, N.N. Adarsh, A. Paul, T.K. Paine, *Inorg. Chem.* 49 (2010) 541–551;
 (e) X. Zhang, B. Liu, A. Liu, W. Xie, W. Chen, *Organometallics* 28 (2009) 1336–1349;
 (f) L. Petit, C. Adamo, N. Russo, *J. Phys. Chem. B* 109 (2005) 12214–12221;
- [25] (g) F. Bernardi, A. Bottoni, I. Rossi, *J. Am. Chem. Soc.* 120 (1998) 7770–7775.
 (a) V.K.K. Praneeth, F. Neese, N. Lehnert, *Inorg. Chem.* 44 (2005) 2570–2572;
 (b) K. Fujisawa, Y. Noguchi, Y. Miyashita, K. Okamoto, N. Lehnert, *Inorg. Chem.* 46 (2007) 10607–10623.
- [26] (c) A.E. Reed, L.A. Curtiss, F. Weinhold, *Chem. Rev.* 88 (1988) 899–926.
- [27] (a) C. Gonzalez, H.B. Schlegel, *J. Chem. Phys.* 90 (1989) 2154–2161;
 (b) H.B. Schlegel, in: J. Bertran (Ed.), *New Theoretical Concepts for Undergraduating Organic Reaction*, Kluwer Academic, The Netherlands, 1989, pp. 33–53.
- [28] (a) M. Cossi, G. Scalmani, N. Rega, V. Barone, *J. Chem. Phys.* 117 (2002) 43–54;
 (b) M. Cossi, V. Barone, R. Cammi, J. Tomasi, *Chem. Phys. Lett.* 255 (1996) 327–335;
 (c) S. Miertus, E. Scrocco, J. Tomasi, *Chem. Phys.* 55 (1981) 117–129.